JOURNAL OF Materials CHEMISTRY

Atomic layer epitaxy growth of $LaGaO_3$ thin films

Minna Nieminen,*[a] Sari Lehto[b] and Lauri Niinistö[a]

[a]*Helsinki University of Technology, Laboratory of Inorganic and Analytical Chemistry, P.O.Box 6100, FIN-02015 Espoo, Finland. E-mail: Minna.Nieminen@hut.fi*
[b]*VTT Chemical Technology, P.O.Box 1404, FIN-02044 VTT, Finland*

Received 5th July 2001, Accepted 8th October 2001
First published as an Advance Article on the web 7th November 2001

Lanthanum gallate thin films were deposited by atomic layer epitaxy (ALE) at 325–425 °C from β-diketonate-type precursors, $La(thd)_3$ and $Ga(acac)_3$, and ozone. Films were grown on soda lime glass, Si(100), MgO-buffered Si(100), sapphire, MgO(100), $SrTiO_3$(100) and $LaAlO_3$(100) substrates. Good control of film stoichiometry was obtained by adjusting the $La(thd)_3/O_3$ to $Ga(acac)_3/O_3$ pulsing ratio. Stoichiometric $LaGaO_3$ films contained only 0.4 at.% carbon and less than 0.2 at.% hydrogen as impurities. Films were transparent and uniform and their thickness could be accurately controlled by the number of deposition cycles. The as-deposited films were amorphous and became crystalline upon annealing. The annealed films grown on sapphire and MgO(100) substrates were polycrystalline $LaGaO_3$ whereas a $La_4Ga_2O_9$ phase was formed when the films grown on Si(100) and MgO-buffered Si(100) were annealed. Epitaxial and smooth $LaGaO_3$ thin films were obtained on $LaAlO_3$(100) after annealing at 850 °C, verified by measurements of the X-ray rocking curve of the (200) reflection and the AFM surface roughness.

Introduction

The ABO_3 perovskite-type oxides have many potential applications for instance as electrodes, sensors, catalysts, superconductors and ferroelectrics. In recent years many studies have shown that the electric and magnetic properties of these materials can be controlled by changing the combination of elements (A, B) and the oxygen stoichiometry.

Since the promising results of Sandstrom *et al.*,[1] many of the studies concerning $LaGaO_3$ have been motivated by its possible use as a substrate for epitaxial high-temperature superconducting (HTS) films.[2,3] As compared to the commonly used $SrTiO_3$ substrate, $LaGaO_3$ has a better lattice match with HTS materials and furthermore its dielectric constant at room temperature ($\varepsilon = 25$) is significally lower than that of $SrTiO_3$ ($\varepsilon = 277$).[2,3] However, the first-order phase transition of $LaGaO_3$ at $\sim$150 °C, from orthorhombic structure to a rhombohedral form,[4,5] has been reported to cause surface roughening, which can be detrimental to the properties of HTS films.[6]

Doped $LaGaO_3$, which was first reported by Ishihara *et al.*,[7] has been extensively examined for use in solid oxide fuel cells (SOFC).[8–12] $LaGaO_3$ doped with Sr at the La-site and with Mg at the Ga-site has been reported to exhibit high oxide ion conductivity.[7,10–12] In addition, electrical conductivity of $LaGaO_3$-based oxides can be improved by doping the Ga-site with Fe, Co or Ni.[8] Mixed electronic–ionic conductors have various applications such as air-separating membranes, electrodes and gas sensors. Recently, Mathews *et al.*[13,14] have extended the research field to Sr and Mg doped $LaGaO_3$ thin film materials.

Many of the applications require that the material is in the form of a thin film, but there are only few reports dealing with the thin film growth of $LaGaO_3$. Morrell *et al.*[15] obtained epitaxial $LaGaO_3$ films on single-crystal $LaAlO_3$(100) substrates by using a sol–gel process followed by post-annealing at 850 °C. Kagawa *et al.*[16] reported the growth of stoichiometric $LaGaO_3$ films at 900 °C by a spray-ICP technique. (112) oriented $LaGaO_3$ films were obtained on sapphire (110) substrates whereas (022) oriented films could be grown on sapphire (001). Randomly oriented $LaGaO_3$ films were obtained on silicon (111) after the films deposited by RF magnetron sputtering were annealed at 900 °C for 30 minutes.[17] To the best of our knowledge, $LaGaO_3$ thin films have not been deposited by chemical vapor deposition (CVD) methods. Heteroepitaxial $NdGaO_3$[18] and $PrGaO_3$[19] have been deposited on single-crystal $LaAlO_3$ substrates by metal organic chemical vapor deposition (MOCVD), but other reports concerning the CVD growth of gallates were not found in the literature.

Our earlier studies showed that perovskite-type oxide thin films such as $LaNiO_3$, $LaCoO_3$, $LaMnO_3$ and more recently $LaAlO_3$ could be deposited by ALE.[20–23] In the present work, we report for the first time the results of a detailed study on the ALE growth of $LaGaO_3$.

Experimental

Film deposition

Films were deposited in a commercial flow-type F-120 ALE-reactor (ASM Microchemistry Ltd, Espoo, Finland).[24] The pressure in the reactor during deposition was 200–300 Pa. The metal precursors, $La(thd)_3$ (thd = 2,2,6,6-tetramethylheptane-3,5-dionate) and $Ga(acac)_3$ (acac = pentane-2,4-dionate) were synthesized applying the method described by Eisentraut and Sievers[25] and Belcher *et al.*,[26] and purified by sublimation. Ozone, used as an oxidizer, was generated from oxygen gas (99.999%) in an ozone generator (Fischer model 502). Nitrogen (>99.999%) obtained from a nitrogen generator (Schmidlin UHPN 3000, Switzerland) was used as a carrier and purging gas. The metal precursors were evaporated inside the reactor from open glass crucibles held at 170 °C for $La(thd)_3$ and 125 °C for $Ga(acac)_3$. The films were grown using the pulsing sequences shown in Table 1. To grow films with different thickness the number of deposition cycles was varied. The pulse times were 0.8 s for the metal precursors and 2 s for ozone with purge times of 2 s. Films were deposited on soda lime glass (5×5 cm^2) and silicon(100) substrates and after optimizing the growth parameters also on sapphire, $SrTiO_3$(100), MgO(100), $LaAlO_3$(100) and MgO-buffered Si(100). MgO buffer layers were grown by the ALE method as described in detail

 DOI: 10.1039/b105978p

Table 1 Pulsing sequences of the source materials for the preparation of $La_xGa_yO_z$ films. The number of deposition cycles (N) was varied depending on the desired film thickness

Sample	Pulsing sequence
1	$N \times [1 \times (La(thd)_3 + O_3) + 3 \times (Ga(acac)_3 + O_3)]$
2	$N \times [1 \times (La(thd)_3 + O_3) + 2 \times (Ga(acac)_3 + O_3)]$
3	$N \times [1 \times (La(thd)_3 + O_3) + 1 \times (Ga(acac)_3 + O_3)]$
4	$N \times [3 \times (La(thd)_3 + O_3) + 2 \times (Ga(acac)_3 + O_3)]$
5	$N \times [2 \times (La(thd)_3 + O_3) + 1 \times (Ga(acac)_3 + O_3)]$
6	$N \times [5 \times (La(thd)_3 + O_3) + 2 \times (Ga(acac)_3 + O_3)]$
7	$N \times [3 \times (La(thd)_3 + O_3) + 1 \times (Ga(acac)_3 + O_3)]$
8	$N \times [5 \times (La(thd)_3 + O_3) + 1 \times (Ga(acac)_3 + O_3)]$

earlier.[27,28] All substrates used were cleaned ultrasonically in ethanol and deionized water before use.

The temperature range available for the growth of $LaGaO_3$ ternary oxide can be determined by the deposition temperatures of the binary oxides La_2O_3 and Ga_2O_3. Self-limited ALE growth of Ga_2O_3 films has been achieved in the temperature range of 350–375 °C.[29] The new experiments using a different ALE reactor showed that the films were uniform even outside the ALE window up to 425 °C. At 300 °C the growth rate was very low and below 300 °C no Ga_2O_3 film formation was detected. In our earlier study[30] uniform La_2O_3 films could be grown in the temperature range 300–425 °C. Based on the data of the constituent oxides, a deposition temperature range of 325–425 °C was chosen for this study.

Selected thin film samples were heat-treated in a rapid thermal annealing furnace PEO 601 (ATV Technologie GmbH, Germany). Annealing was carried out in nitrogen atmosphere for 10–30 minutes at temperatures between 800–950 °C.

Characterization

Thicknesses and refractive indices of the films were determined by fitting the measured optical spectra as described by Ylilammi and Ranta-aho.[31] Depending on the substrate type, either reflectance or transmittance spectra were measured with a Hitachi U-2000 double beam spectrophotometer in the region of 190–1100 nm for silicon substrates and 370–1100 nm for soda lime glass. AFM measurements were carried out by using a Nanoscope III atomic force microscope (Digital Instruments) operated in tapping mode with a scan rate of 1–2 Hz. To obtain representative images of the surface, wide areas (10×10 μm^2) were scanned at different parts of the sample before the scan size was reduced to 2×2 μm^2 to record the final image. Roughness values were calculated as root mean square values (rms).

Film crystallinity was determined by a Philips powder diffractometer MPD 1880 using Cu K_α radiation. Rocking curve measurements were performed with a Bruker axs D8 Advance diffractometer using parallel beam geometry.

Two complementary ion beam techniques, Rutherford backscattering spectrometry (RBS) and time-of-flight elastic recoil detection analysis (TOF-ERDA) were used to determine the film composition and stoichiometry. The RBS experiments were carried out with $^4He^+$ ions from the 2.5 MV Van de Graaff accelerator operated at 3.0 MeV. A scattering angle of 170° was used. A beam of $^{197}Au^{9+}$ ions at 48 MeV for TOF-ERDA was obtained from a 5 MV tandem accelerator EGP-10-II. The sample surface was tilted 20° and recoils were detected at an angle of 40° with respect to the incoming beam.

The La and Ga contents were also determined with a Philips PW 1480 X-ray fluorescence spectrometer equipped with a Rh X-ray tube. Data analysis was performed with the UNIQUANT 2.5 program, which utilises a DJ Kappa model to calculate the composition and mass thickness of an unknown bulk or thin film sample.[32] The XRF analysis results were calibrated by plotting the XRF La/Ga ratio against the La/Ga ratio measured by RBS and TOF-ERDA.

Surface composition of the films was determined by X-ray photoelectron spectroscopy (XPS) with a Kratos Analytical AXIS 165 spectrometer using monochromated Al K_α radiation. Since ion bombardment is known to degrade chemical information, no sputter cleaning was performed. For elemental identification, wide binding energy spectra of 0–1100 eV were recorded at 80 eV analyser pass energy and a 1 eV step. For surface chemical analysis, high-resolution regional spectra of La 3d, Ga 2p, O 1s and C 1s were recorded using 20 eV analyser pass energy and 0.1 eV steps. The charge build-up due to the insulating sample matrix was neutralized with slow thermal electrons during the data acquisition.[33] The binding energies were corrected afterwards using the C–C bond in the C 1s signal at 285.0 eV as an internal standard.[34]

Depth profiles of lanthanum, gallium, carbon, silicon and magnesium were measured with a VG IX70S double focusing magnet sector secondary ion mass spectrometer. The 3 keV O_2^+ primary ion beam was rastered over an area of 300×400 μm^2 while the primary ion current was 100 or 150 nA. The detected area was limited to 10% by electronic gating to avoid crater wall effects. The secondary ion currents of $^{12}C^+$, $^{24}Mg^+$, $^{29}Si^+$, $^{69}Ga^+$ and $^{139}La^+$ were recorded at low mass resolution.

Results and discussion

As-deposited films

In the first set of experiments, various La : Ga precursor pulsing ratios were studied at four temperatures, 325 °C, 350 °C, 370 °C and 410 °C. The film composition, as determined by XRF, RBS and TOF-ERDA, was linearly related with the precursor pulsing ratio at all temperatures studied, see Fig. 1. The stoichiometric composition was achieved in the deposition temperature range of 350–390 °C with a pulsing ratio of 2.5, *i.e.* 5 to 2, see Fig. 1 inset. Because of the linear relation between the film composition and the precursor pulsing ratio, stoichiometric $LaGaO_3$ films can be produced at any deposition temperature between 325 and 425 °C by selecting a suitable precursor pulsing ratio. The deposition temperature of 370 °C was chosen for more detailed studies.

Deposition of the films was very reproducible. All films with different La : Ga atomic ratios were of uniform thickness both along and across the gas flow direction. The growth rate of stoichiometric $LaGaO_3$ films of various thicknesses deposited at 370 °C on soda lime and silicon substrates with the La : Ga precursor pulsing ratio of 2.5 was constant, as shown in Fig. 2.

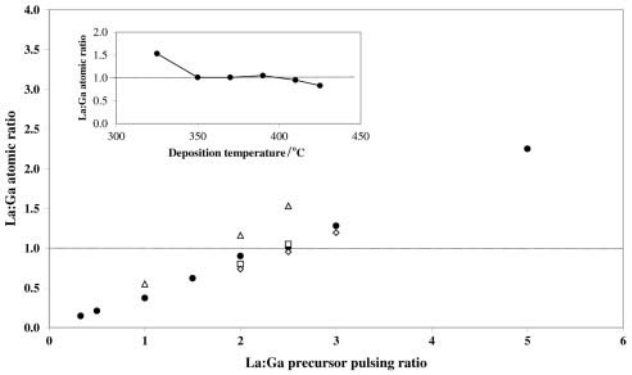

Fig. 1 La : Ga atomic ratio in $La_xGa_yO_z$ films deposited on silicon(100) substrates at 325 °C (△), 350 °C (□), 370 °C (●) and 410 °C (◊) as a function of the $La(thd)_3/O_3$ to $Ga(acac)_3/O_3$ cycle ratio. The film composition was measured by XRF and independently verified by RBS and TOF-ERDA. Inset shows the La : Ga atomic ratio of the films deposited with a La : Ga precursor pulsing ratio of 2.5 as a function of deposition temperature.

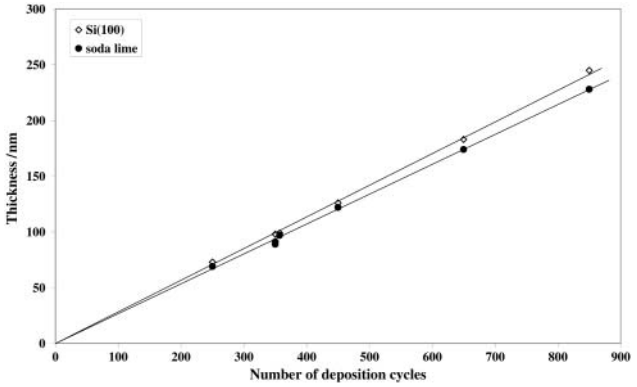

Fig. 2 The dependence of the $LaGaO_3$ film thickness on the number of deposition cycles at 370 °C. The films were grown on silicon(100) and soda lime glass substrates using the La : Ga precursor pulsing ratio of 2.5.

The film growth rate was 0.38 Å per cycle on soda lime glass substrate and a slightly higher 0.40 Å per cycle on silicon. XRF measurements showed that the La : Ga atomic ratio over the area of two substrates, *i.e.* 10×5 cm^2, and the composition in films of various thicknesses remained constant, indicating that the growth was well controlled.

Since the growth rate of lanthanum oxide at 370 °C is greater than that of gallium oxide,[29,30] the growth rate of $La_xGa_yO_z$ should increase with the increasing number of $La(thd)_3/O_3$ cycles. However, the film growth rate at 370 °C was rather constant at different La : Ga pulsing ratios up to 5.0 and the growth rate relative to that of the separate oxides clearly decreased, see Fig. 3. A similar effect was earlier seen in the thin film ALE growth process of $LaAlO_3$.[23] These phenomena might be explained by inhibition of the growth of the La–O layer by the previously formed Ga–O or Al–O surface. Possibly, either the surface sites available are not favourable for the adsorption of $La(thd)_3$ or the bonding mode of $La(thd)_3$ on the Ga–O surface differs from that on the La–O surface.

All as-deposited films were amorphous and the AFM measurements showed that the $LaGaO_3$ films grown on silicon(100) were smooth, the AFM roughness values being around 0.5 nm, see Fig. 4a. The depth distributions of lanthanum and gallium in $LaGaO_3$ films deposited on silicon and MgO-buffered silicon substrates were uniform as recorded in the SIMS profiles of Figs. 5a and c. This is consistent with the RBS data of a $LaGaO_3$ film deposited on silicon, where uniform distribution was also detected. The interfaces of $LaGaO_3$–silicon and $LaGaO_3$–MgO were well defined and no diffusion could be detected.

TOF-ERD analysis of the $La_xGa_yO_z$ films deposited onto Si(100) showed that the films contained small amounts of the

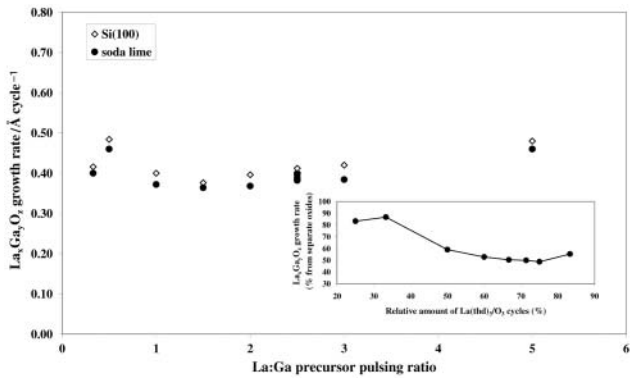

Fig. 3 The growth rate of $La_xGa_yO_z$ films deposited at 370 °C on soda lime glass and silicon(100) substrates as a function of pulsing ratio of $La(thd)_3/O_3$ to $Ga(acac)_3/O_3$.

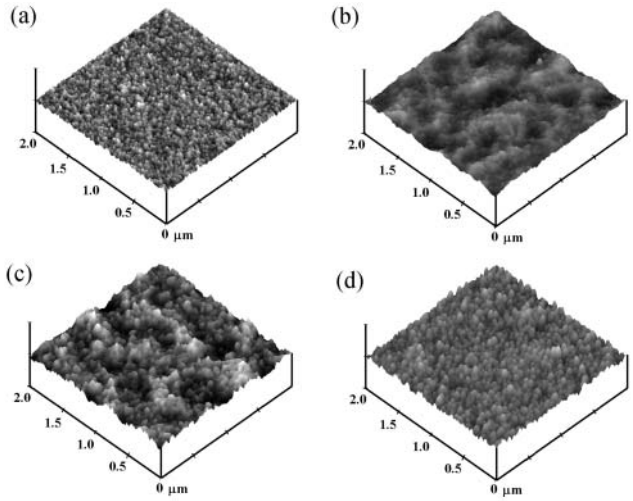

Fig. 4 AFM images of the $LaGaO_3$ thin film surfaces. 100 nm thick film grown on silicon(100): a) as-deposited amorphous film, rms = 0.5 nm, b) annealed at 850 °C in N_2 for 30 minutes, rms = 0.9 nm and c) annealed at 950 °C in N_2 for 30 minutes, rms = 1.9 nm. d) 100 nm thick film deposited on $LaAlO_3$(100) and annealed at 850 °C in N_2 for 30 minutes, rms = 1.1 nm. Image size: 2 μm × 2 μm. Depth scale: 20 nm from black to white.

common impurities, carbon and hydrogen. In addition fluorine contamination was detected, possibly due to the use of Teflon gaskets or perfluorinated vacuum greases. The films with a stoichiometric La : Ga atomic ratio contained about 0.4 at.% carbon, less than 0.2 at.% hydrogen and less than 0.3 at.% fluorine. A decrease in carbon impurity level from 1.0 at.% to 0.2 at.% was observed when the La : Ga atomic ratio in the films was decreased from 2.3 to 0.2. This could mean that carbon is mainly related to the La–O part of the film.

In the high-resolution XPS spectra of stoichiometric $LaGaO_3$ films the peaks of La $3d_{5/2}$ at 835.3 ± 0.5 eV and Ga 2p at 1118 eV ± 0.5 were detected. The La $3d_{5/2}$ and $3d_{3/2}$ core-level peaks were both split into two components which has also been reported for La_2O_3, $LaAlO_3$ and other mixed oxides of

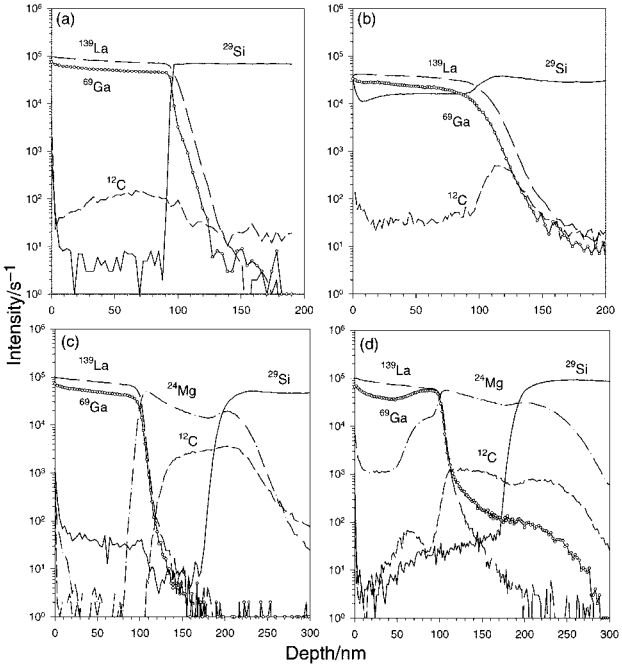

Fig. 5 SIMS depth profiles of the $LaGaO_3$ thin films. 100 nm thick film grown on silicon(100): a) as-deposited amorphous film and b) annealed at 950 °C in N_2 for 30 minutes. 100 nm thick film grown on MgO-buffered silicon(100): c) as-deposited amorphous film and d) annealed at 850 °C in N_2 for 30 minutes.

lanthanum.[35–38] The oxygen signal (O 1s) consisted of two resolvable components at 531.7 ± 0.5 eV and at 530.2 ± 0.5 eV. The first component agrees well with the tabulated values of adsorbed O^- and OH^- groups, often detected on air-exposed oxide surfaces, while the second component is characteristic for O^{2-} in an oxide lattice and is in good accordance with the reported values for many mixed oxides of lanthanum.[36–38]

All films grown at different deposition temperatures on soda lime glass substrates were transparent in the wavelength region of 370–1100 nm. Refractive indices of the stoichiometric $LaGaO_3$ films were approx. 1.95 (at 580 nm). When the La : Ga atomic ratio in the films decreased the refractive indices of the films also slightly decreased towards 1.9 for films with the La : Ga atomic ratio around 0.2. Similarly, a small decrease in the refractive index down to 1.9 was detected on films with La : Ga ratio above 1.0.

Annealed films

All as-deposited films were amorphous and therefore post-annealing was needed to obtain crystalline $LaGaO_3$. Stoichiometric $LaGaO_3$ films deposited on Si(100), MgO-buffered Si(100), sapphire, MgO(100), $SrTiO_3$(100) and $LaAlO_3$(100) substrates using the optimized growth parameters at 370 °C were annealed at temperatures between 800–950 °C.

Silicon(100) substrate

All films annealed at 800 °C were still amorphous, but annealing at 850 °C and above in N_2 for 10 minutes produced highly crystalline films. The XRD patterns of annealed films contained peaks, which were identified as of a $La_4Ga_2O_9$ phase,[39] see Fig. 6. Some of the minor peaks can also be identified as those of $LaGaO_3$ phase. According to RBS data, 10 at.% of silicon were found on the surface of a 100 nm thick $La_xGa_yO_z$ film annealed at 950 °C. The SIMS depth profile, presented in Fig. 5b, shows that silicon has diffused through the film, which was further confirmed by XPS wide binding energy spectra. The composition of the film changed with depth. The La : Ga atomic ratio, as determined by RBS, was nearly stoichiometric on the surface of the film, but towards the interface the gallium content decreased with the increasing silicon content, the La : Ga atomic ratio reaching 1.5 in the bulk of the film.

The binding energies of the La $3d_{5/2}$ and Ga 2p lines in XPS high-resolution spectra of the film annealed at 950 °C remained unaffected by annealing. However, a small change in the shape of the La $3d_{5/2}$ and $3d_{3/2}$ peaks was detected, possibly due to subtle changes in the valence band caused by changes in the La coordination number before and after annealing, as discussed by Burroughs *et al.*[38] A similar phenomenon has been observed in our earlier studies of $LaNiO_3$ and $LaAlO_3$ films.[20,23]

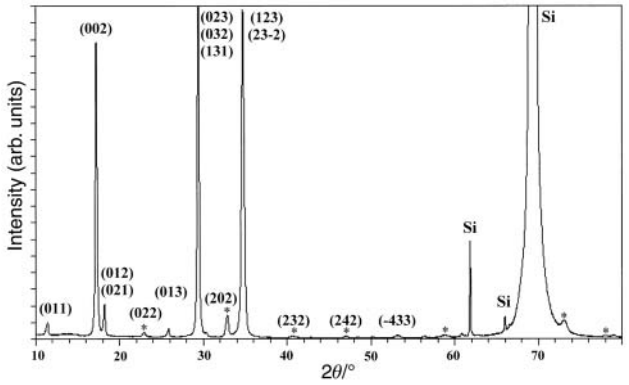

Fig. 6 XRD pattern of a 100 nm thick $La_xGa_yO_z$ film grown on an Si(100) substrate and annealed at 850 °C in N_2 for 30 minutes. Miller indices of $La_4Ga_2O_9$ are given.[39] Possible peaks of $LaGaO_3$ phase are marked with an asterisk (*).

The surface morphology of films grown on Si(100) substrates and annealed at temperatures between 800–950 °C was analyzed by AFM. The films had a smooth surface and the AFM surface roughness changed from 0.5 nm to 1.9 nm when the annealing temperature was increased from 800 °C to 950 °C, see Fig. 4b and c. The columnar-type structure seen in the AFM images of the annealed $La_xAl_yO_z$ films[23] was not observed in the AFM images of the $La_xGa_yO_z$ films.

MgO-buffered silicon(100) substrate

$LaGaO_3$ films were deposited on MgO-buffered Si(100) substrates to study whether the observed mixing of the silicon substrate and the $LaGaO_3$ film could be prevented. Furthermore, in our earlier study the orientation of $LaAlO_3$ films could be controlled by using oriented MgO layers.[23] The ALE-grown MgO buffer layers that have either preferred (100) or (111) orientation were employed.[27,28] The as-deposited $LaGaO_3$ films grown on MgO-buffered silicon were stoichiometric and amorphous but became crystalline upon annealing in nitrogen at 850 °C for 10 minutes. In the XRD patterns peaks originating from the $La_4Ga_2O_9$ phase were seen in a similar way as in the XRD patterns of films grown on Si(100) and annealed at the same temperature. Also the XPS high-resolution spectra were similar to the spectra measured for an annealed film deposited on silicon.

According to RBS data, the La : Ga ratio in the films annealed at 850 °C was not constant throughout the film, varying from around 1.35 at the top layer of the film to around 1.0 near the interface. The decrease in the lanthanum content and the increase in the gallium content towards the $La_xGa_yO_z$–MgO interface was also seen in the SIMS depth profile, see Fig. 5d. No diffusion of silicon through the MgO buffer layer into the $La_xGa_yO_z$ layer was observed in the SIMS depth profile and silicon was not detected in the $La_xGa_yO_z$ layer by RBS either. However, magnesium has diffused through the $La_xGa_yO_z$ film, which was further confirmed by XPS data where weak Mg KLL lines were observed in spectra of this specimen. Magnesium was not detected in the bulk of the $La_xGa_yO_z$ film by RBS, most probably because detection of magnesium by RBS is not sensitive enough. Both RBS and SIMS data showed, however, that an intermediate layer exists where lanthanum, gallium and magnesium were mixed.

In our earlier study on the deposition of $LaAlO_3$ films on silicon or MgO-buffered silicon,[23] the formation of the $La_4Al_2O_9$ phase, identified by the XRD patterns, was observed only at a higher annealing temperature of 950 °C. The effect was most obvious when the MgO layer thickness or that of the $LaAlO_3$ film was below 100 nm. In the $LaGaO_3$ case, however, $La_4Ga_2O_9$ phase was formed on silicon and MgO-buffered silicon irrespective of the annealing temperature or the MgO layer and $LaGaO_3$ film thickness. The formation of the $Nd_4Ga_2O_9$ phase rather than the expected $NdGaO_3$ phase has been reported in the study of Čečkauskas *et al.*,[40] where Nd–Ga–O films were deposited at 750 °C on Si(100) and Si(111) substrates by rf-magnetron sputtering. They concluded that the formation of the $Nd_4Ga_2O_9$ phase on silicon takes place due to silicon oxide, which is formed on the silicon surface during film deposition. Recently, Sammes *et al.*[9] reported that Ga-site doping of $LaGaO_3$ with Mg leads to the formation of a $La_4Ga_2O_9$ secondary phase. In our studies, the formation of $La_4Al_2O_9$ or $La_4Ga_2O_9$ phases was detected when either silicon or magnesium was diffused into the $LaAlO_3$ or $LaGaO_3$ films. Therefore we believe that this kind of diffusion initiates the formation of the $La_4X_2O_9$ (X = Al, Ga) phase.

The La : Ga atomic ratio in the bulk of the annealed films deposited on silicon or MgO-buffered silicon determined by

RBS differed from the La : Ga ratio of the $La_4Ga_2O_9$ phase observed by XRD. Probably part of the gallium is in the form of amorphous oxide on grain boundaries and therefore not detected by XRD. It is also noteworthy that the diffusion of silicon or magnesium into the $LaGaO_3$ film occurred at a considerably lower temperature than in the case of $LaAlO_3$.[23] Therefore it seems that silicon and magnesium diffuse more easily into the $LaGaO_3$ film than into the $LaAlO_3$ film. More work is needed to identify the cause of the stronger interaction of Si and Mg with $LaGaO_3$ than with $LaAlO_3$ observed in the present study.

Single-crystal oxide substrates

Failing to produce crystalline $LaGaO_3$ phase on either silicon or MgO-buffered silicon substrates, films were deposited on single-crystal substrates, sapphire and MgO(100). Lattice-matching perovskite-type substrates *viz.* $SrTiO_3$(100) and $LaAlO_3$(100) were also employed to study whether epitaxial $LaGaO_3$ films can be obtained.

Polycrystalline $LaGaO_3$ films, with the (112) reflection being the most intense, were obtained when the as-deposited amorphous films on sapphire and single-crystal MgO(100) substrates were annealed at 850 °C or above in nitrogen atmosphere, see Fig. 7. Increasing the annealing time from 10 to 30 minutes did not have any effect on the crystal orientation. It is interesting to note that the same annealing procedure led to the formation of a polycrystalline $LaGaO_3$ phase when films were deposited on single-crystal MgO(100) whereas the films deposited on MgO-buffered silicon crystallized as the $La_4Ga_2O_9$ phase. Our results suggest that the ALE-grown MgO film was not stable enough at high annealing temperatures, probably because the MgO film is polycrystalline.

The as-deposited films grown on $SrTiO_3$(100) and $LaAlO_3$(100) were amorphous but became crystalline upon annealing at 850 °C and above for 10 to 30 minutes. The degree of crystallinity was enhanced when a longer annealing time and slower heating and cooling rates were used. Fig. 8 shows the XRD pattern of the $LaGaO_3$ film grown on $LaAlO_3$(100) and annealed at 850 °C for 30 minutes. The three peaks observed, in addition to the (100), (200) and (300) $LaAlO_3$ reflections, can be identified as the (100), (200) and (300) reflections of the $LaGaO_3$ perovskite structure (using the pseudocubic indexing of $LaGaO_3$ and $LaAlO_3$). The rocking curve scan of the (200) $LaGaO_3$ reflection of a film deposited on $LaAlO_3$(100) is shown in the inset of Fig. 8. The full-width at half-maximum (FWHM) value of 0.183° proves that the $LaGaO_3$(100) film on $LaAlO_3$(100) is of high quality and epitaxial. Furthermore, the surface roughness was only 1.1 nm, as determined by AFM, see Fig. 4d.

Since the difference of the lattice constants of $LaGaO_3$ and

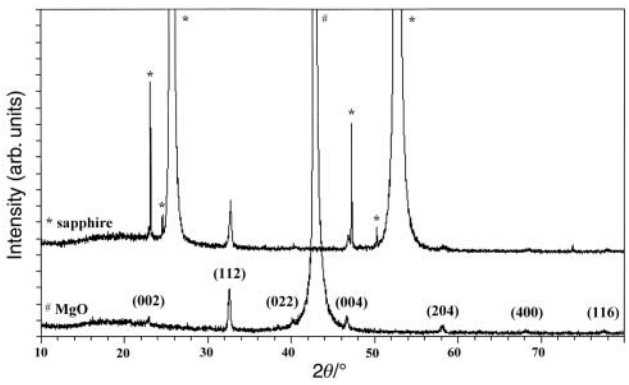

Fig. 7 XRD patterns of 100 nm thick $LaGaO_3$ films grown on sapphire or MgO(100) substrates and annealed at 850 °C in N_2 for 30 minutes. Diffraction peaks are identified according to JCPDS card 24-1102.

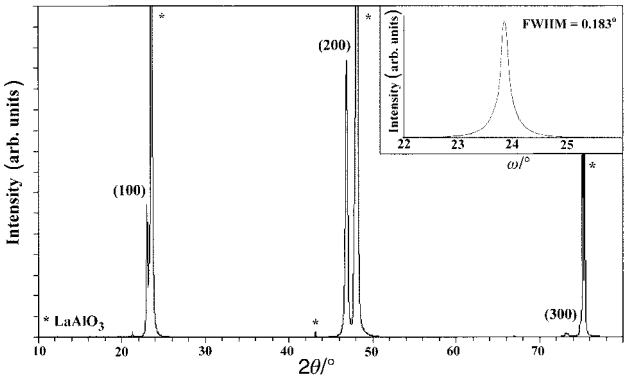

Fig. 8 XRD pattern of an epitaxial $LaGaO_3$ film grown on $LaAlO_3$-(100). The film was 100 nm thick and it was annealed at 850 °C in N_2 for 30 minutes. Inset shows the rocking curve of the (200) reflection of $LaGaO_3$ (FWHM = 0.183°).

$SrTiO_3$ is very small, peaks due to the $LaGaO_3$ film were difficult to separate from the $SrTiO_3$ peaks. Only a small (300) reflection of $LaGaO_3$ was detected at $d = 1.29$ Å and the (100) and (200) reflections were not resolved. Despite this, the absence of the XRD peaks of randomly oriented $LaGaO_3$ strongly suggests that $LaGaO_3$ can be heteroepitaxially grown on $SrTiO_3$(100) by ALE using the process presented in this study.

The best samples of $LaGaO_3$ films were obtained on matching perovskite substrates. A similar phenomenon has been reported in other studies as well and was also seen in our results on $LaAlO_3$ thin film deposition. It is understandable that epitaxial growth is achieved rather on lattice-matched substrates and the non-lattice matched substrates will give rise to randomly or slightly oriented films.

Conclusions

We have demonstrated for the first time the ALE growth of $LaGaO_3$ thin films on soda lime glass, Si(100), MgO-buffered Si(100), sapphire, MgO(100), $LaAlO_3$(100) and $SrTiO_3$(100) using β-diketonate-type precursors, $La(thd)_3$ and $Ga(acac)_3$, and ozone. It is shown that stoichiometric $LaGaO_3$ films can be obtained at deposition temperatures between 325 and 425 °C when a suitable La : Ga precursor pulsing ratio is selected.

The film growth was reproducible and the films were uniform with only small thickness variations of 1–6% over the substrate area of 10×5 cm^2. A linear dependence of the film thickness on the number of deposition cycles was observed, typical of a self-limiting ALE growth mechanism. Also the film stoichiometry was maintained with the increasing thickness, thus verifying good control of the process. The stoichiometric $LaGaO_3$ films contained only 0.4 at.% carbon and less than 0.2 at.% hydrogen as impurities.

The as-deposited films were amorphous on all substrates but crystallized upon annealing at 850 °C under nitrogen atmosphere. An interdiffusion between the silicon substrate and the $LaGaO_3$ film as well as between the ALE-grown MgO buffer layer and the $LaGaO_3$ film occurred at all annealing temperatures resulting in the formation of a $La_4Ga_2O_9$ phase. Polycrystalline $LaGaO_3$, with the (112) reflection being the most intense one, was obtained on sapphire and single-crystal MgO(100) substrates at 850 °C and above. High quality, epitaxial and smooth $LaGaO_3$ thin films were obtained on $LaAlO_3$(100) after annealing at 850 °C, verified by the X-ray rocking curve of the (200) reflection having a full-width at half-maximum (FWHM) of 0.183° and by the AFM surface roughness of 1.1 nm.

Acknowledgements

The authors wish to thank Dr. Eero Rauhala and Mr. Timo Sajavaara at the Accelerator Laboratory of the University of Helsinki for the RBS and TOF-ERDA analysis, respectively. Thanks are also due to Mr. Jaakko Niinistö at Helsinki University of Technology for the AFM measurements and to Mr. Antti Niskanen at the University of Helsinki for the rocking curve measurements. Furthermore, Dr. Joseph Campbell and Dr. Leena-Sisko Johansson at the HUT Center for Chemical Analysis are thanked for the XPS analyses and fruitful discussions.

References

1 R. L. Sandstrom, E. A. Giess, W. J. Gallagher, A. Segmüller, E. I. Cooper, M. F. Chisholm, A. Gupta, S. Shinde and R. B. Laibowitz, *Appl. Phys. Lett.*, 1988, **53**, 1874.
2 J. M. Phillips, *J. Appl. Phys.*, 1996, **79**, 1829.
3 E. A. Giess, R. L. Sandstrom, W. J. Gallager, A. Gupta, S. L. Shinde, R. F. Cook, E. I. Cooper, E. J.M. O'Sullivan, J. M. Roldan, A. P. Segmüller and J. Angilello, *IBM J. Res. Dev.*, 1990, **34**, 916.
4 L. Vasylechko, A. Matkovski, A. Suchocki, D. Savytskii and I. Syvorotka, *J. Alloys Compd.*, 1999, **286**, 213.
5 C. J. Howard and B. J. Kennedy, *J. Phys. Condens. Matter*, 1999, **11**, 3229.
6 S. Miyazawa, *Appl. Phys. Lett.*, 1989, **55**, 2230.
7 T. Ishihara, H. Matsuda and Y. Takita, *J. Am. Chem. Soc.*, 1994, **116**, 3801.
8 T. Ishihara, T. Yamada, H. Arikawa, H. Nishiguchi and Y. Takita, *Solid State Ionics*, 2000, **135**, 631.
9 N. M. Sammes, G. A. Tompsett, R. J. Phillips and A. M. Cartner, *Solid State Ionics*, 1998, **111**, 1.
10 D. Lybye, F. W. Poulsen and M. Mogensen, *Solid State Ionics*, 2000, **128**, 91.
11 J. Drennan, V. Zelizko, D. Hay, F. T. Ciacchi, S. Rajendran and S. P. S. Badwal, *J. Mater. Chem.*, 1997, **7**, 79.
12 T. Ishihara, J. A. Kilner, M. Honda and Y. Takita, *J. Am. Chem. Soc.*, 1997, **119**, 2747.
13 T. Mathews, J. R. Sellar, B. C. Muddle and P. Manoravi, *Chem. Mater.*, 2000, **12**, 917.
14 T. Mathews, P. Manoravi, M. P. Antony, J. R. Sellar and B. C. Muddle, *Solid State Ionics*, 2000, **135**, 397.
15 J. S. Morrell, Z. B. Xue, E. D. Specht and D. B. Beach, *Mater. Res. Soc. Symp. Proc.*, 1999, **547**, 309.
16 M. Kagawa, M. Arimura, M. Nagano and Y. Syono, *Adv. Sci. Technol.(Faega, Italy, Surface Eng.)*, 1999, **20**, 241.
17 X. F. Meng, F. S. Pierce, K. M. Wong, R. S. Amos, C. H. Xu, B. S. Deaver Jr. and S. J. Poon, *IEEE Trans. Magn.*, 1991, **27**, 1638.
18 B. Han, D. Neumayer, D. L. Schulz, T. J. Marks, H. Zhang and V. P. Dravid, *Appl. Phys. Lett.*, 1992, **61**, 3047.
19 B. Han, D. A. Neumayer, T. J. Marks, D. A. Rudman, H. Zhang and V. P. Dravid, *Appl. Phys. Lett.*, 1993, **63**, 3639.
20 H. Seim, H. Mölsä, M. Nieminen, H. Fjellvåg and L. Niinistö, *J. Mater. Chem.*, 1997, **7**, 449.
21 H. Seim, M. Nieminen, L. Niinistö, H. Fjellvåg and L-S. Johansson, *Appl. Surf. Sci.*, 1997, **112**, 243.
22 O. Nilsen, M. Peussa, H. Fjellvåg, L. Niinistö and A. Kjekshus, *J. Mater. Chem.*, 1999, **9**, 1781.
23 M. Nieminen, T. Sajavaara, E. Rauhala, M. Putkonen and L. Niinistö, *J. Mater. Chem.*, 2001, **11**, 2340.
24 T. Suntola, *Thin Solid Films*, 1992, **216**, 84.
25 K. J. Eisentraut and R. E. Sievers, *J. Am. Chem. Soc.*, 1965, **87**, 5256.
26 R. Belcher, C. R. Jenkins, W. I. Stephen and P. C. Uden, *Talanta*, 1970, **17**, 455.
27 M. Putkonen, L-S. Johansson, E. Rauhala and L. Niinistö, *J. Mater. Chem.*, 1999, **9**, 2449.
28 M. Putkonen, T. Sajavaara and L. Niinistö, *J. Mater. Chem.*, 2000, **10**, 1857.
29 M. Nieminen, L. Niinistö and E. Rauhala, *J. Mater. Chem.*, 1996, **6**, 27.
30 M. Nieminen, M. Putkonen and L. Niinistö, *Appl. Surf. Sci.*, 2001, **174**, 155.
31 M. Ylilammi and T. Ranta-aho, *Thin Solid Films*, 1993, **232**, 56.
32 *UniQuant Version 2 User Manual*, Omega Data Systems, Neptunus 2, NL-5505 Veldhoven, The Netherlands, 1994.
33 *Axis 165, Operating Manual and User's Guide*, Kratos Analytical Ltd, Manchester, 1995.
34 G. Beamson and D. Briggs, *High Resolution XPS of Organic Polymers, The Scienta ESCA300 Database*, John Wiley & Sons, Chichester, England, 1992.
35 *Handbook of X-ray Photoelectron Spectroscopy*, eds. J. Chastain and R. C. King Jr., Physical Electronics, Eden Prairie, Minnesota, 1995.
36 P. A. W. van der Heide and J. W. Rabalais, *Chem. Phys. Lett.*, 1998, **297**, 350.
37 C.-M. Pradier, C. Hinnen, K. Jansson, L. Dahl, M. Nygren and A. Flodström, *J. Mater. Sci.*, 1998, **33**, 3187.
38 P. Burroughs, A. Hamnett, A. F. Orchard and G. Thornton, *J. Chem. Soc., Dalton Trans.*, 1976, 1686.
39 *Joint Committee on Powder Diffraction Standards*, Card 37-1433, JCPDS, International Center for Diffraction Data, Newtown Square, Pennsylvania, USA.
40 I. Čečkauskas, E. Šatkovskis and U. O. Karlsson, *Liet. Fiz. Z.*, 1997, **37**, 494.